Removal of Cd(II) from aqueous solution with activated Firmiana Simplex Leaf: Behaviors and affecting factors

Qiang Tang[a], Xiaowu Tang[a,*], Manman Hu[b], Zhenze Li[c,*], Yunmin Chen[a], Peng Lou[a]

[a] MOE Key Laboratory of Soft Soils and Geoenvironmental Engineering, Department of Civil Engineering, Zhejiang University, Yuhangtang Road 388, Hangzhou, 310058, PR China
[b] Department of Civil & Environmental Engineering, Duke University, Durham, NC, USA
[c] GSGES, Kyoto University, Kyoto, Japan

ABSTRACT

Cadmium pollution is known to cause severe public health problems. This study is intended to examine the effect of an activated Firmiana Simplex Leaf (FSL) on the removal of Cd(II) from aqueous solution. Results showed that the active Firmiana Simplex Leaf could efficiently remove Cd(II) from wastewater due to the preservation of beneficial groups (amine, carboxyl, and phosphate) at a temperature of 250 °C. The adsorbent component, dosage, concentration of the initial solute, and the pH of the solution were all found to have significant effects on Cd(II) adsorption. The kinetic constants were predicted by pseudo-first-order kinetics, and the thermodynamic analysis revealed the endothermic and spontaneous nature of the adsorption. FT-IR and XRD analyses confirmed the strong adsorption between beneficial groups and cadmium ions, and the adsorption capacity was calculated to be 117.786 mg g^{-1} according to the Langmuir isotherm.

© 2010 Elsevier B.V. All rights reserved.

1. Introduction

Recently, the presence of heavy metals in the aquatic environment has attracted the attention because of their toxicity, accumulation in the food chain, and persistence in nature [1–4]. These toxic metals are released into the environment in numerous ways, including from painting, mining drainage, car manufacturing, smelters and metal refineries, and industrial and domestic sewage [5–7].

Cadmium is frequently used in metallurgical alloying, ceramics, metal plating, photograph development, pigment works, textile printing industries, lead–zinc mining, alkaline batteries, and electroplating [8,9]. By the early 1990s, statistical calculations indicated that the worldwide cadmium release rate had reached 22,000 tons/year [10]. Cadmium is not biodegradable [11] and is likely to cause a number of acute and chronic disorders, such as itai-itai disease; renal damage; emphysema; hypertension; testicular atrophy [12]; damage to the kidneys, lungs, and liver [13]; and carcinogenesis [14]. Therefore, the maximum concentration limit for Cd(II) in drinking water has been strictly regulated. The World Health Organization (WHO) and the American Water Works Association (AWWA) have recommended that the concentration of cadmium in drinking water should not exceed 0.005 mg L^{-1}.

The conventional methods for removing heavy metals include precipitation, oxidation, adsorption, coagulation, evaporation, membrane filtration, and extraction. Among these, adsorption has been the most widely used because it is an economically feasible, versatile, effective, simple, and environmentally friendly method in practice [15–18]. Biosorption has been the focus of recent research for the removal of heavy metals [19–24].

Most Firmiana Simplex grows in areas of medium latitudes, such as Europe, the U.S., Japan, and China. Every autumn, the mass of fallen leaves must be swept up, landfilled, incinerated, or incubated [25]. Due to the limited capacity of landfills and harmful emissions during incineration, the Firmiana Simplex Leaf (FSL) was utilized as a potentially promising adsorbent in this study. The behaviors of the adsorption of Cd(II) on the adsorbent were evaluated by considering a variety of factors, and the governing mechanisms are assessed and discussed in this paper. Furthermore, investigation of the environmental character of FSL would deepen and broaden our understanding of its viability as an adsorbent for Cd(II).

2. Materials and methods

2.1. Preparation of the adsorbent

The FSL was acquired from Hangzhou, China, in October 2008, oven dried at 45 °C overnight, and then pulverized to pass through

* Corresponding authors. Tel.: +86 571 88208781/+81 75 753 5116; fax: +86 571 85023966/+81 75 753 5116.
E-mail addresses: tangxiaowu@zju.edu.cn (X. Tang), lazyhero@live.cn (Z. Li).

a 24-mesh screen with diameters of $355 \pm 13\,\mu$m. The stock solution of Cd(II) at analytical reagent grade was prepared by dissolving $Cd(NO_3)_2$ (Sinopharm, China) in de-ionized water to reach the target concentration. Conical flasks and polyvinyl chloride (PVC) centrifuge tubes were immersed in a $0.01\,mol\,L^{-1}$ HNO_3 solution overnight and then rinsed three times with de-ionized water.

The FSL powder was placed in an oven ($15\,cm \times 25\,cm \times 40\,cm = 15,000\,cm^3$). The oven was sealed except for a 0.5-cm-diameter hole to allow any volatile emissions to escape. The temperature was separately regulated at 150, 200, 250, 300, and 350 °C with an increment of 25–30 °C/min, and then the powder was kept for 5 h. Once the treatment duration was reached, the product was cooled to room temperature, after which the activated ashes that remained were collected and stored for further study.

2.2. Characterization

FT-IR spectra of the samples before and after adsorption were recorded using a Nexus-670 FT-IR spectrophotometer (Nicolet Corporation, USA) to study changes in the functional groups in order to investigate the mechanism of Cd(II) adsorption. The Cd(II)-laden leaf sample (400 mg) was first equilibrated with 40 mL of $5\,g\,L^{-1}$ Cd(II) solution for 24 h at 55 °C and then centrifuged from the mixture at 3000 rpm for 5 min. The supernatants were discarded and replaced by fresh de-ionized water to decrease or remove Cd(II) from the solution and further to obtain theoretical Cd(II)-laden samples without disturbance. The mixture was intensely stirred for 5 min and then separated by centrifugation. The sediments were collected and cleaned two more times. After that, the Cd(II)-laden adsorbent was dried under infrared radiation for 10 min, encapsulated in KBr, ground into fine powder in a carnelian mortar, compressed into a translucent slice at a pressure of 40 MPa, and finally exposed to infrared radiation to determine the functional groups.

The pH values of the samples were determined by a PHS-25 glass electrode potentiometer (Precision Scientific Instrument Co. Ltd., China), following the method used by previous researchers [26]. XRD patterns of Activated Leaf (AL) and Cd(II)-laden leaf were obtained by a D/MAX-RA revolving target X-ray diffraction apparatus (Rigaku Corporation, Japan). The Cd(II)-laden leaf samples were treated following the above-mentioned processes. The cadmium content of the AL was determined by Atomic Absorption Spectroscopy (AAS) (Hitachi Corporation, Japan) following complete digestion of a 1-g sample in 10 mL of a 1:1 mixture of HF/HNO_3.

2.3. Experiment

2.3.1. Adsorption isotherms and thermodynamics

The AL samples ($10\,g\,L^{-1}$) obtained at various treatment temperatures were separately blended with eight sets of cadmium solutions with increasing initial Cd(II) concentrations of 25, 50, 100, 200, 300, 400, 500, and $600\,mg\,L^{-1}$ at 25 °C. All samples were equilibrated for 24 h in the temperature-controlled agitator, and the equilibrium Cd(II) concentrations were measured by an atomic absorption spectrophotometer (AAS). Control tests and parallel tests were conducted, and the results were averaged.

The equilibration temperatures for the most promising adsorbent (obtained at 250 °C in this study) were 5–55 °C at increments of 10 °C in order to investigate the thermodynamic adsorption behaviors. Apart from this, some samples with other initial concentrations (0.8, 1, 2, and $5\,g\,L^{-1}$) at 55 °C were also tested in order to obtain more information about adsorption capacity. Other processes followed the previous tests.
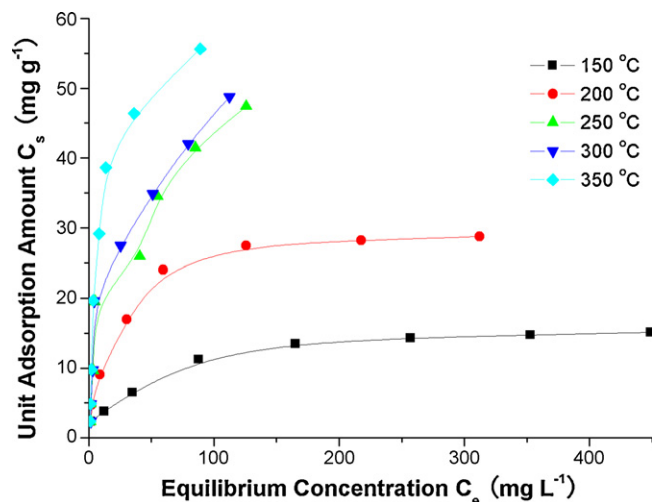

Fig. 1. Isothermal adsorption lines (25 °C) under different calcination temperatures.

2.3.2. Effect of adsorbent dosage

In order to investigate the effect of adsorbent dosage, the adsorbent dosages of AL in the aqueous solution were 0.5, 1, 2, 5, 10, and $20\,g\,L^{-1}$, and each solution was mixed with three different initial Cd(II) concentrations (50, 100, and $200\,mg\,L^{-1}$), which were prepared earlier and placed in stoppered conical flasks. Then, the flasks were put into a thermostatic agitator (25 °C) for 24 h at 180 rpm without pH adjustment. The supernatants were obtained by centrifugation at 3000 rpm for 5 min, then subjected to AAS analysis to determine the Cd(II) concentration. Adsorption on the inner surface of the flasks was evaluated by a series of parallel blank tests using a control and averaging the results.

2.3.3. Adsorption kinetics

The Cd(II) solutions had concentrations of 50, 100, and $200\,mg\,L^{-1}$, while the AL adsorbent dosage was fixed at $10\,g\,L^{-1}$ in this test. The reaction temperature was maintained constant at 25 °C without pH regulation. The test durations were 3, 6, 9, 12, 15, 20, 40, 60, 120, 180, 240, 360, and 420 min. Afterward, the mixture was transferred to PVC tubes and centrifuged at 3000 rpm for 3 min. The Cd(II) concentration in the supernatant was determined by AAS. In addition, duplicate and blank tests were conducted to obtain an average value for each test.

2.3.4. Effect of pH

The adsorbent and Cd(II) solutions were separately mixed in nine pretreated PVC tubes, with the parameters fixed as follows: dosage = $10\,g\,L^{-1}$ and initial Cd(II) concentration = $100\,mg\,L^{-1}$. Then, pH values of the initial solution of the samples were modified, ranging from 2.0 ± 0.2 to 10.0 ± 0.2 in increments of 1.0 by adding $0.1\,mol\,L^{-1}$ HCl or NaOH solution. After that, these samples were placed into a thermostatic agitator (25 °C) and rotated at 180 rpm for 24 h. Finally, the pH values of the solutions were measured.

The supernatants were obtained through centrifugation at 3000 rpm for 5 min and then sampled to determine the Cd(II) concentration by AAS. All experiments were conducted in duplicate.

3. Results and discussion

3.1. Adsorption isotherms at different temperatures

Fig. 1 shows isothermal adsorption (25 °C) at different calcination temperatures. Fig. 2 shows the adsorption isotherms of Cd(II) on AL at different equilibration temperatures (calcination temperature = 250 °C). A gradual ascending trend for unit adsorption
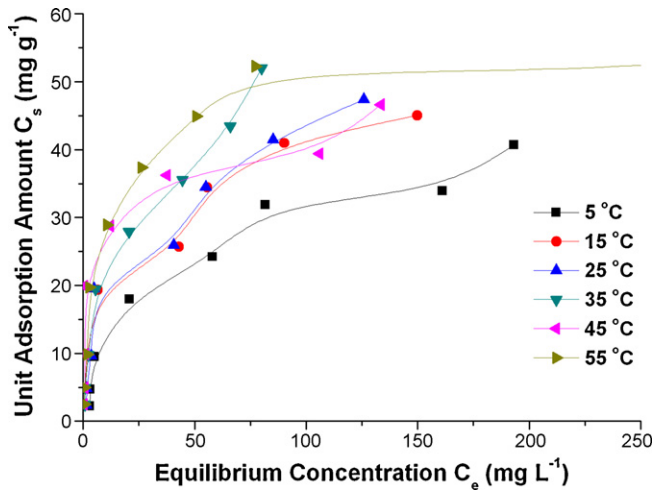
Fig. 2. Isothermal adsorption lines under different temperatures (calcination temperature = 250 °C).
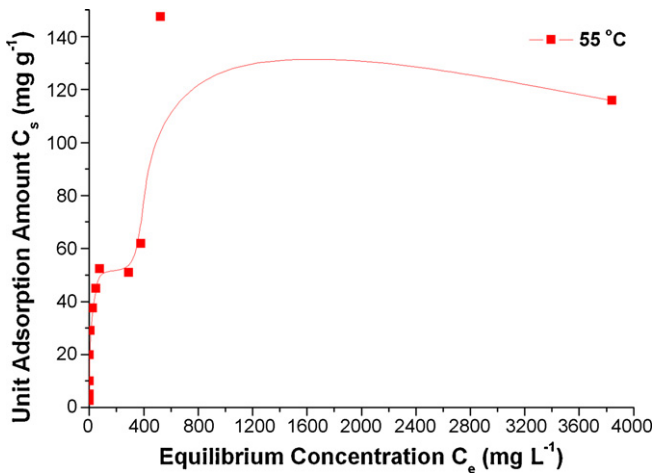

Fig. 3. Isothermal adsorption lines under temperature 55 °C.

amount was observed, and, eventually, a maximum adsorption amount was achieved with increasing equilibrium solute concentrations. Thus, it could be predicted that the unit adsorption amount would not increase any more after the adsorbent reached its ultimate adsorption amount, as shown in Fig. 3. Three general isothermal equations, including the Langmuir, Freundlich, and D–R (Dubinin–Radushkevich) models, were used to evaluate the test

results in order to obtain more information about the adsorption mechanisms.

The Langmuir isotherm can be written as [27]:

$$\frac{1}{C_s} = \frac{1}{Q^0} + \frac{1}{bQ^0C_e}, \tag{1}$$

where C_e is the equilibrium concentration of solute solution $(\mathrm{mg\,L^{-1}})$, Q^0 is the maximum adsorption capacity of the adsorbent $(\mathrm{mg\,g^{-1}})$, and b $(\mathrm{L\,mg^{-1}})$ is the Langmuir constant.

The Freundlich model stipulates that the ratio of solute adsorbed to the solute concentration is a function of the solution. The empirical model was shown to be consistent with the exponential distribution of active centers and characteristic of heterogeneous surfaces. The Freundlich isotherm can be expressed as:

$$C_s = K_F C_e^{1/n}, \tag{2}$$

where K_F is the Freundlich constant $(\mathrm{mg\,g^{-1}})$ indicating the adsorption capacity and strength of the adsorptive bond, and n is the heterogeneity factor.

The D–R model assumes a uniform, pore-filling sorption and can predict the free sorption energy change [28–30]. The D–R model is written as:

$$\ln\ C_s = \ln q_m - k\varepsilon^2, \tag{3}$$

where q_m is the maximum adsorption capacity $(\mathrm{mol\,g^{-1}})$, k is a model constant related to the free sorption energy, and ε is the Polanyi potential, which is written as

$$\varepsilon = RT \ln\left(1 + \left(\frac{1}{C_e}\right)\right) \tag{4}$$

The mean free energy of adsorption (E) is:

$$E = -\frac{1}{\sqrt{2k}} \tag{5}$$

The results of predicted isothermal constants for the adsorption of Cd(II) are shown in Table 1. The Langmuir model produced the best fit of the test data based on the correlation coefficients $(R \geq 0.97)$. Sari and Tuzen also concluded that the parameters calculated by the Langmuir model were more accurate than those produced by other models [31]. With respect to the Langmuir isotherm, the adsorption was uniformly distributed among the active sites of the adsorbent, and, once adsorbate occupies a site, no further adsorption can take place at this site [32]. The correlation coefficients between the test data and the fitted curves predicted by the Freundlich and D–R models were reasonably high, close to 1.00, implying that these models could be used to help explain the adsorption performances under particular circumstances.

Table 1
Predicted constants of isothermal models for Cd(II) adsorption.

AL (250 °C)							AL (150 °C)	AL (200 °C)	AL (300 °C)	AL (350 °C)
Adsorption temperature (°C)	5	15	25	35	45	55	25	25	25	25
Langmuir model										
Q^0 $(\mathrm{mg\,g^{-1}})$	45.147	46.620	52.632	54.915	45.475	117.786	16.210	30.665	55.340	66.138
b $(\mathrm{L\,mg^{-1}})$	0.027	0.076	0.044	0.071	0.167	0.012	0.029	0.053	0.046	0.065
R	0.981	0.984	0.973	0.980	0.994	0.992	0.998	0.999	0.977	0.970
Freundlich model										
K_F $(\mathrm{mg\,g^{-1}})$	2.296	5.290	3.780	4.785	8.203	7.375	1.809	2.780	3.813	4.738
n	1.751	2.180	1.819	1.788	2.621	2.492	2.721	2.178	1.741	1.515
R	0.943	0.959	0.929	0.967	0.857	0.931	0.985	0.959	0.921	0.905
D–R model										
q_m $(\mathrm{mg\,g^{-1}})$	172.554	142.938	210.105	246.585	125.551	190.263				
k $(\mathrm{mol^2\,kJ^{-2}})$	0.0063	0.0043	0.005	0.0045	0.0029	0.0034				
E $(\mathrm{kJ\,mol^{-1}})$	−8.909	−10.783	−10.000	−10.541	−13.131	−12.127				
R	0.953	0.972	0.940	0.976	0.869	0.960				
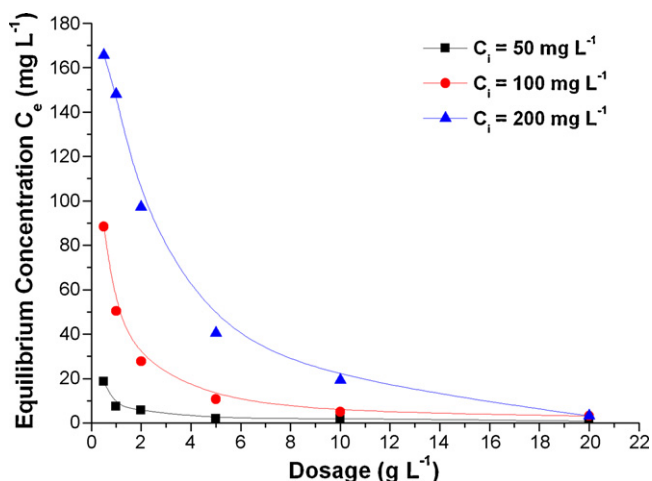
Fig. 4. Variation of equilibration concentration with the dosage.

Fig. 5. The effect of dosage on unit adsorption amount.

Based on the test results, it is obvious that 250 °C is an effective activation temperature. The Langmuir adsorption capacities of the five adsorbents obtained at 150, 200, 250, 300, and 350 °C for Cd(II) were 16.2, 30.7, 52.6, 55.3, and 66.1 mg g^{-1}, respectively. Increased activation temperatures directly resulted in increased Cd(II) adsorption capacity. The increase was sharp within the range of 150–250 °C, but little benefit was obtained when the temperature was increased in the range of 300–350 °C, as shown in Fig. 1. At treatment temperatures around 250 °C, an increase of 50 °C just resulted in an increase of 2.7 mg g^{-1} in Cd(II) adsorption. Therefore, we considered 250 °C as the most suitable treatment temperature in this study.

From the analysis with the Langmuir model, the maximum Cd(II) adsorption capacities of AL (250 °C) were estimated to be 45.147, 46.620, 52.632, 54.915, 45.475 and 117.786 mg g^{-1} at equilibration temperatures increasing from 5 to 55 °C, respectively. Similar to the work of Unuabonah et al., this study shows that the adsorption capacity peaked at the highest temperature [33]. The parameter n of the Freundlich model ranged from 1.751 to 2.621 at different temperatures, indicating a highly heterogeneous surface and multi-layered adsorption.

The adsorption capacities estimated by the D–R model were 172.554, 142.938, 210.105, 246.585, 125.551 and 190.263 mg g^{-1} at temperatures from 5, 15, 25, 35, 45 and 55 °C, respectively. These values were considerably higher than those obtained by the Langmuir model since the inherent assumption of the D–R model is that all the micropores are available to the solute. This is an ideal state that cannot be achieved in practice. Following the D–R theory, the adsorption is basically a surface adsorption associated with ion exchange when $|E|$ is between 8 and 16 kJ mol^{-1}, whereas, for $|E|$ in the range of 1.0–8.0 kJ mol^{-1}, the mechanism is physical adsorption [34,35]. Thus, it could be speculated that there is a chemical bond between the adsorbent and Cd(II), because most of the absolute values of estimated free adsorption energy were around 10 kJ mol^{-1}.

3.2. Effect of adsorbent dosage

The effect of adsorbent dosage is shown in Fig. 4. Based on these results, the Cd(II) removal efficiencies of the AL adsorbent were calculated, and they are shown in Fig. 5. It is apparent that, although the amounts of Cd(II) removed increased with increasing dosage (Fig. 1), the unit adsorption amount decreased continually from 68.9 to 49.65 mg g^{-1}, and 62.6 to 9.84, 4.84, and 2.46 mg g^{-1}, respectively (Fig. 5) as a result of less availability to adsorbent. This trend was not linear, because the sharp decrease in the first stage (0.5 g L^{-1} < dosage < 10 g L^{-1}) was interrupted and gradually leveled
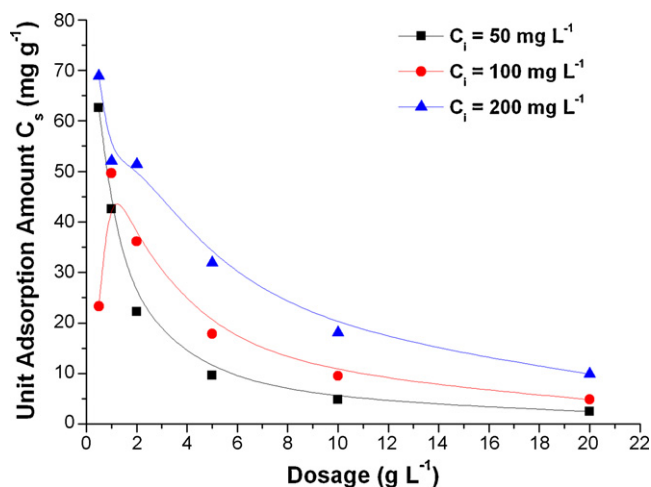
at higher dosage (dosage >10 g L^{-1}), similar to the results obtained in earlier studies [36–40].

Comparing Fig. 4 with Fig. 5, the total removal percent and the unit adsorption amount of the adsorbent appeared to change with dosage in a contradictory manner. Thus, there is a need to find an optimum adsorbent dosage to satisfy both the total Cd(II) uptake and the adsorption efficiency. Based on the trend of the variation of C_e (equilibrium concentration) of Cd(II) solution and C_s (unit adsorption amount), the optimum adsorbent dosage was determined to be 10 g L^{-1}, and this concentration was used in subsequent experiments.

3.3. Adsorption kinetics

The variation of the equilibrium concentration of Cd(II) with the equilibration duration at different initial solute concentrations is shown in Fig. 6. It is obvious that the reaction equilibrated very quickly. The duration required for reaching adsorption equilibrium increased with increasing initial Cd(II) concentration, e.g., equilibrium was reached in only 6 min when C_i was 50 mg L^{-1}, but it took about 20 min when C_i was 200 mg L^{-1}. However, it is noteworthy to mention that the duration required to reach equilibrium in this study was far less than those of other adsorbents in previous studies [41,42].
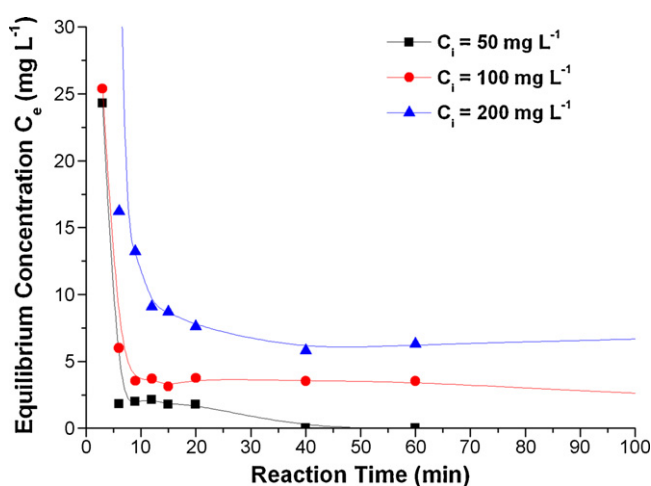

Fig. 6. Variation of equilibrium concentration of Cd(II) with equilibration duration.
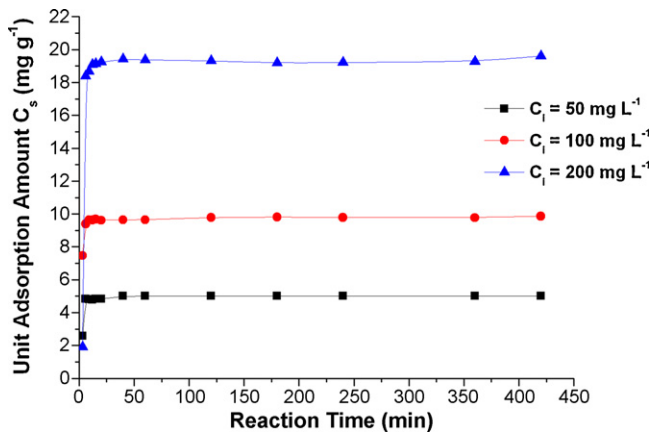
Fig. 7. Effect of duration on the unit adsorption amount.

Fig. 7 shows C_s of Cd(II) on the AL adsorbent as a function of equilibration durations. The plot indicates a two-step adsorption process, which consisted of a rapid adsorption process and a slow adsorption step during which equilibrium was obtained. The unit adsorption amount of Cd(II) reached a relatively high value within a fairly short time period (about 10 min from 0 to 18.36, 9.4, and 4.82 mg g^{-1}), and then it slowly increased until it reached a plateau after 20 min. The test data were further analyzed with three kinetic models (a pseudo-first-order kinetic model, a pseudo-second-order kinetic model, and the intra-particle diffusion model), as follows:

The pseudo-first-order kinetic equation is [43]:

$$log(Q_e - C_s) = log(C_e) - \frac{k_1}{2.303}t, \qquad (6)$$

where Q_e and C_s are the amounts of solute adsorbed per unit adsorbent at equilibrium and any time (mg g^{-1}), respectively, and k_1 is the pseudo-first-order rate constant (min^{-1}).

The pseudo-second-order kinetic equation is [43]:

$$\frac{t}{C_s} = \frac{1}{k_2 Q_e^2} + \frac{1}{Q_e}t, \qquad (7)$$

where k_2 is the pseudo-second-order rate constant (g mg^{-1} min^{-1}).

The equation for the intra-particle diffusion model is [43]:

$$C_s = k_{int}t^{1/2} + C, \qquad (8)$$

where k_{int} is the relevant rate constant (mg g^{-1} min$^{-1/2}$), and C is the intercept.

Table 2 lists the critical parameters of adsorption kinetics. According to the correlation coefficient (R^2) value listed in the table, the pseudo-first-order kinetics equation ($R^2 = 0.879$, 0.979, and 0.720) could better fit the test data than the pseudo-second-order kinetics equation ($R^2 = 0.709$, 0.795, and 0.566).

Table 2
Predicted kinetic constants of Cd(II) adsorption on activated leaf.

C_i (mg L^{-1})	50	100	200
The pseudo-first-order kinetics equation			
Q_e (mg g^{-1})	4.992	9.743	19.710
k_1 (min^{-1})	0.313	0.494	0.207
R^2	0.879	0.979	0.720
The pseudo-second-order kinetics equation			
k_2 (g mg^{-1} min^{-1})	0.127	0.143	0.017
Q_e (mg g^{-1})	5.165	9.940	20.623
R^2	0.709	0.795	0.566
The intra-particle diffusion model			
k_{int} (mg g^{-1} min$^{-1/2}$)	0.042	0.044	0.260
C	4.374	9.139	15.583
R^2	0.177	0.211	0.126

In addition, there was a slight decrease in the rate constant k_1 from 0.313 to 0.207 g mg^{-1} min^{-1} when the initial Cd(II) concentration was increased from 50 to 200 mg L^{-1}. This indicates that a solution with a lower solute concentration is likely to equilibrate much faster. This is consistent with the previously observed Zn(II) adsorption on Chinese loess [44]. The predicted adsorption amounts per unit mass were 4.992, 9.743 and 19.710 mg g^{-1} by the pseudo-first-order kinetics for solutions with initial Cd(II) concentrations of 50, 100, and 200 mg L^{-1}, respectively.

3.4. Thermodynamics

For the sake of studying the thermodynamic behaviors of Cd(II) adsorption, thermodynamic considerations was evaluated. Thermodynamic parameters such as enthalpy change (ΔH°), Gibbs free energy change (ΔG°), and entropy change (ΔS°) can be estimated with the following Gibbs free energy equations:

$$\Delta G^\circ = -RT \ln K_D, \qquad (9)$$

$$\Delta G^\circ = \Delta H^\circ - T\Delta S^\circ, \qquad (10)$$

where R is the ideal gas constant (8.314 J mol^{-1} K^{-1}), T is the absolute temperature (K), and K_D is the distribution coefficient of the solute between the adsorbent and the solution in equilibrium C_s/C_e (mL g^{-1}).

Eqs. (9) and (10) can be written in linearized form between K_D and $1/T$ as:

$$\ln K_D = \frac{\Delta S^\circ}{R} - \frac{\Delta H^\circ}{RT}, \qquad (11)$$

Values of ΔH° and ΔS° can be determined from the slope and the intercept of the plot between $\ln K_D$ versus $1/T$ [45,46].

The predicted constants of thermodynamics shown in Table 3 can be determined through linearization of the test data, as shown in Fig. 8. The correlation coefficients were less than 0.80 at $C_i = 25$ and 100 mg L^{-1}, but they were larger than 0.80 at $C_i = 50$ and
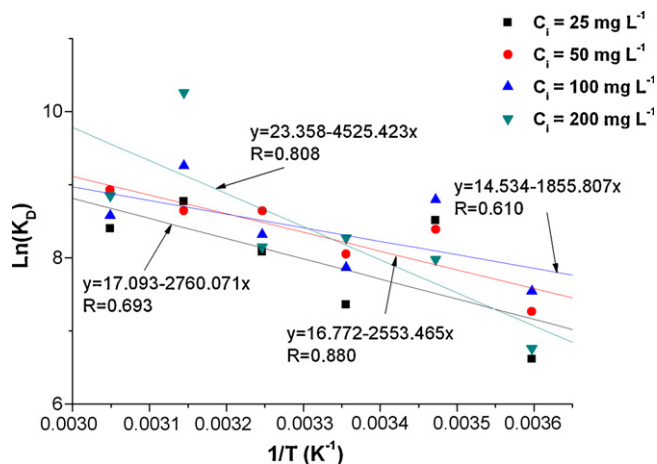
Table 3
Thermodynamic parameters for adsorption of Cd(II) on activated leaf.

C_i (mg L^{-1})		25		50		100		200	
Temperature (°C)	$1/T$	$\ln K_D$	G° (kJ mol^{-1})	$\ln K_D$	G° (kJ mol^{-1})	$\ln K_D$	G° (kJ mol^{-1})	$\ln K_D$	G° (kJ mol^{-1})
5	0.003597122	6.613	−15.284	7.263	−16.787	7.539	−17.425	6.759	−15.621
15	0.003472222	8.511	−20.380	8.386	−20.079	8.789	−21.045	7.975	−19.096
25	0.003355705	7.357	−18.227	8.047	−19.938	7.864	−19.484	8.269	−20.486
35	0.003246753	8.081	−20.694	8.640	−22.125	8.316	−21.294	8.143	−20.852
45	0.003144654	8.766	−23.175	8.642	−22.849	9.256	−24.472	10.257	−27.117
55	0.00304878	8.400	−22.906	8.927	−24.344	8.575	−23.383	8.842	−24.112
ΔS° (J mol^{-1} K^{-1})		142.110		139.440		120.837		194.192	
ΔH° (kJ mol^{-1})		22.947		21.230		15.429		37.624	
R		0.693		0.880		0.610		0.808	

Fig. 8. Fitting test data with Gibbs free energy equations.

Fig. 10. Variation of equilibrium pH (pH_e) under different initial solution pH (pH_i).

$200 \, mg \, L^{-1}$. Accordingly, the latter two series of test data are used in the following discussions. The calculated Gibbs free energy decreased as reaction temperature increased at a fixed initial solute concentration. At initial solute concentrations ranging from 50 to $200 \, mg \, L^{-1}$, the Gibbs free energy was negative, approximating the results of Lin and Juang [47], which suggested that the adsorption process was spontaneous and could be promoted by increasing the temperature. This could also explain the phenomenon that the adsorption capacity peaked at the highest temperature. The values of the adsorption enthalpy changes extrapolated in this study (21.230 and $37.624 \, kJ \, mol^{-1}$), which approached the value of $39.52 \, kJ \, mol^{-1}$ that was published by Yavuz et al. [48], implying that the adsorption process was endothermic and implied an increasing disorder in the system (the change of entropy: 139.440 and $194.192 \, J \, mol^{-1} \, K^{-1}$).

3.5. Effect of pH

Fig. 9 shows the Cd(II) adsorption percent of the AL adsorbent versus the initial solution pH (pH_i). The pH values of the solutions were influenced significantly by the amounts of Cd(II) that were adsorbed on the AL adsorbent. A sharp pH-adsorption edge was observed between pH 3.0 and 6.0, while the Cd(II) removal percentage increased from 0% to 94.8%, and the curve then flattened at almost 100% Cd(II) removal with continuously increasing pH_i values. Almost all of the cadmium had been removed from the solution near neutral conditions (pH_i around 6.0). Therefore, raising
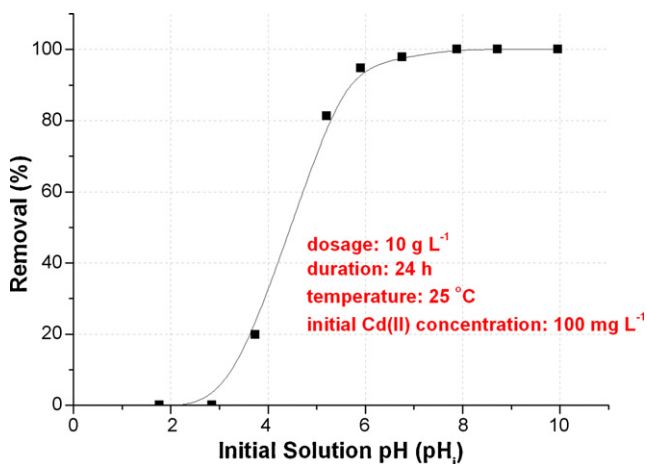
the solution pH to maintain a neutral or alkaline solution would promote the adsorption of Cd(II) by the adsorbent.

Fig. 10 shows that the equilibrium pH (pH_e) values lie approximately above the diagonal line for $pH_i < 5.21$, on the diagonal line for $5.21 < pH_i < 6.28$, and below the diagonal line for $pH_i > 6.28$. It is obvious that the AL adsorbent has good buffering capability, which means it can effectively resist the pH changes in solution. The change of pH_e might reflect the inherent mechanism that governs the adsorption of Cd(II) on the AL adsorbent, particularly regarding the effect of solution pH.

4. Discussion of adsorption mechanism

The FT-IR bands of the adsorbent before and after Cd(II) adsorption were taken in the range of $400–4000 \, cm^{-1}$, as shown in Fig. 11, to obtain information on the adsorption mechanism. The relevant functional groups on the samples could be determined based on the FT-IR adsorption band listed in Table 4. The weak band intensity of the CH group at $2920 \, cm^{-1}$, as shown in Fig. 11(a), means that the content of the CH group is very low after activation at $250 °C$. The natural macromolecules (i.e., lignin) contained in the FSL, which remain stable even after mulched for 2 months [49], were greatly decomposed in this respect.

According to the FT-IR test, the bands at 475, 1319, and $1620 \, cm^{-1}$ could be regarded as bending vibrations of N–H group

Fig. 9. Variation of Cd(II) removal percentage with varied initial solution pH (pH_i).

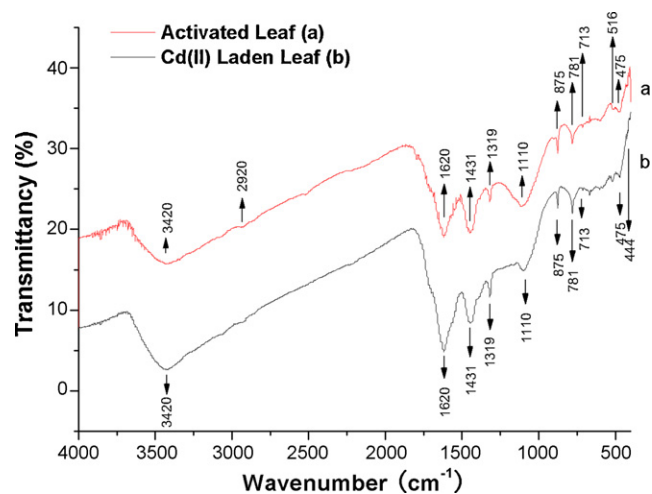**Fig. 11.** IR spectra of activated leaf and Cd(II)-laden leaf ((a) Activated Leaf; (b) Cd(II)-laden leaf).

Table 4
Band position in the FT-IR spectra.

Sample		Assignment	Reference
Activated leaf	Cd(II)-laden leaf		
875	875	C=O	
475	475	N–H	[50]
713	713	C=O	[53]
781	781	Si–O	
1319	1319	N–H	
3420	3420	O–H	[55]
1110	1110	C=O	
1620	1620	N–H	
516		P–O	[54]
2920	2920	C–H	

[50]. As an alkaline functional group, amine could raise the solution pH, corresponding to the fact that the equilibrium pH of the adsorbent/water slurry $(10\,g\,L^{-1})$ was higher than 8.60 in this study. However, the deprotonated amine group would turn to possess positive charges at pH < 2.0. This behavior might reduce the Cd(II) adsorption capacity significantly, which could explain the minor removal percent (almost 0%) at solution pH 2.85 and the sharp pH-adsorption edge between 3.0 and 6.0 observed in Fig. 9. Amine was found in both samples, but the band intensity of N–H in the Cd(II)-laden leaf shown in Fig. 11(b) decreased greatly after adsorption $(475\,cm^{-1})$ compared to the AL adsorbent, indicating the decreased percent of the N–H group in the Cd(II)-laden leaf. According to previous research, the amine group was reported as a significant binding site for metal uptake in biosorbents [51]. The high affinity of amine for Cd(II) would contribute to the adsorption of Cd(II) on the AL adsorbent. Specifically, the disappearance of some N–H group indicated the following reaction:

$$S - NH_2 + Cd^{2+} \rightarrow \ S - NHCd^+ + H^+ \tag{12}$$
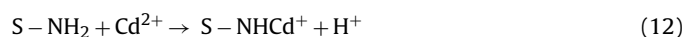
Eq. (12) would be also helpful to explain why pH always dropped $(pH_i > pH_e)$ after Cd(II) adsorption, especially when pH > 6.28. In Fig. 11(b), function group such as O–H $(3420\,cm^{-1})$ remained stable according to their band intensities.

The bands at 1431, 1110, and $875\,cm^{-1}$ were observed before and after adsorption, and these bands were considered to result from a carboxyl group in the form of organic matter or carbonate, which provided a preferential adsorption site for heavy metals [26]. The weak band at $713\,cm^{-1}$ was relevant either to hydrogen bonding with the vanadyl group [52] or to carbonate components [53]. In the XRD patterns, as shown in Fig. 12, calcite was observed
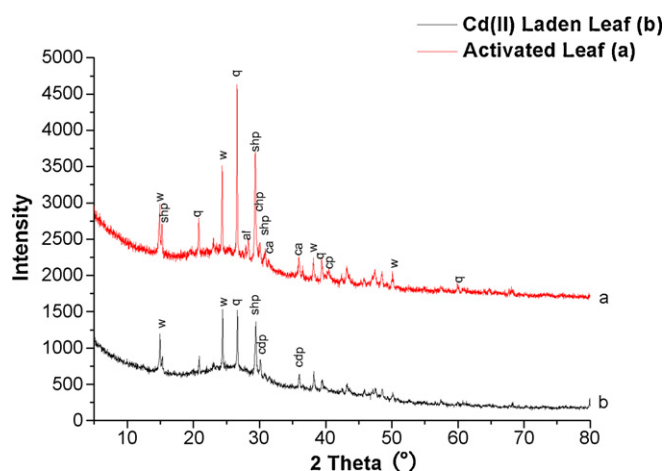

Fig. 12. XRD spectra of (a) activated Leaf and (b) Cd(II)-laden leaf [w: whewellite, q: quartz, shp: sodium hydrogen phosphate hydrate, cp: calcium phosphate, al: albite, chp: calcium hydroxide phosphate, ca: calcite, cdp: cadmium phosphate].

according to the characteristic peaks at $2\theta = 31.4°$, and 35.9°, consistent with the presence of the carboxyl group in the IR spectra, indicating the possible interaction modes:
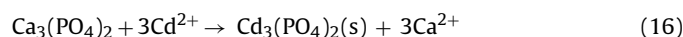
$$-COOH + Cd^{2+} \rightarrow \ -COOCd^+ + H^+ \tag{13}$$
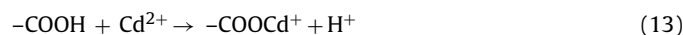
The carbonate component, i.e., the calcite identified by the XRD patterns $(2\theta = 31.4°$ and 35.9°) in Fig. 12, was hardly seen after Cd(II) adsorption. Assuming that the calcite had been proved to be an effective adsorbent for removing heavy metals from solutions [26], the adsorption of Cd(II) on the AL adsorbent might be written as:

$$CaCO_3 + Cd^{2+} \rightarrow \ CdCO_3(s) + Ca^{2+} \tag{14}$$
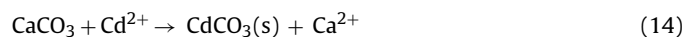
This is a chemical adsorption and could be linked to the results of D–R analysis (the least adsorption energy $(-8.909\,kJ\,mol^{-1})$, indicating the presence of chemical adsorption). In view of the weak intensities of the IR band and XRD patterns relevant to carbonate in the original AL adsorbent, the carbonate contained in the AL adsorbent, while it contributes to Cd(II) adsorption, might not be the dominant adsorption site.

In Fig. 11(a), the IR band at $516\,cm^{-1}$ relevant to phosphate [54] was also observed in the AL adsorbent, implying that a proper activation temperature (around $250\,°C$) was beneficial to preserve the originally contained phosphor element in the leaf [51]. In addition, characteristic peaks at $2\theta = 15.23°$, 29.4°, 30.1°, and 30.88° in the XRD pattern, as shown in Fig. 12, were attributed to sodium hydrogen phosphate hydrate and calcium hydroxide phosphate. Calcium phosphate was also present in the AL adsorbent according to the relevant peak at $2\theta = 40.53°$, corresponding to the bands of phosphate observed in Fig. 11.

New peaks were observed at $2\theta = 30.14°$ and 36.0°, compared to the original AL adsorbent, while some peaks at $2\theta = 20.8°$, 26.6°, 39.4°, 59.96°, 29.4°, 30.1°, 40.53°, and 30.88° weakened or disappeared when the AL adsorbent was laden with Cd(II). The peaks at $2\theta = 30.14°$ and 36.0° could be attributed to $Cd_3(PO_4)_2$. The formation of $Cd_3(PO_4)_2$ and the change in the characteristic peak intensity of phosphate (at $2\theta = 29.4°$, 30.1°, 30.88°, and 40.53°, as exhibited in Fig. 12) suggest the adsorption of Cd(II) in the following forms:

$$MHPO_4 + Cd^{2+} \rightarrow \ CdHPO_4(s) + M^{2+} \tag{15}$$

$$Ca_3(PO_4)_2 + 3Cd^{2+} \rightarrow \ Cd_3(PO_4)_2(s) + 3Ca^{2+} \tag{16}$$

The component of $MHPO_4$ in the adsorbent was soluble. It is noteworthy to mention that if the cation M were magnesium, the Eq. (15) reaction would become insignificant with respect to its comparatively low dissolution coefficients.

Furthermore, some other main minerals in the AL adsorbent, such as quartz, whewellite, and albite, were determined from the characteristic peaks in the XRD pattern. (See Fig. 12.) In Fig. 12(a), the peaks at $2\theta = 14.9°$, 24.5°, 38.1°, and 50.1° could be assigned to whewellite (calcium oxalate hydrate). The peak at $2\theta = 24.5°$ was sharp and strong, indicating that this crystalline component was well preserved at $250\,°C$.

In addition, quartz (silicon dioxide) possibly played an important part in metal adsorption due to the relatively weakened characteristic peaks in XRD pattern (at $2\theta = 20.8°$, 26.6°, 39.4°, and 59.96°), in agreement with the decreasing IR bands (Si–O at $781\,cm^{-1}$), as shown in Fig. 11. As mentioned above, the natural pH of the AL adsorbent is above 8.60. Under strong alkaline conditions, some SiO_2 could hydrolyze to form SiO_3^{2-}, and then the combination of SiO_3^{2-} and Cd^{2+} could form $CdSiO_3$, which helped to immobilize soluble Cd(II) from solutions. The reactions could be written as:

$$SiO_2 + H_2O \rightarrow \ SiO_3^{2-} + 2H^+ \tag{17}$$

$$SiO_3^{2-} + Cd^{2+} \rightarrow \ CdSiO_3 \tag{18}$$

Table 5
Reported adsorption capacity of Cd(II) on various adsorbents.

Materials	Predicted adsorption capacity (mg g^{-1})	Reaction duration	Reference
Carbonized coirpith	93.2	40 min	[20]
Bagasse	54	About 5 h	[56]
Areca	1.12	30 min	[57]
Olive cake	10.560	20–30 min	[58]
Olive stone waste	7.73	100 min	[59]
Peat	50.247	60 min	[60]
Activated Firmiana Simplex Leaf (250 °C)	117.786	About 10 min	This study

Various biosorbents have been investigated with respect to their Cd(II) adsorption performance. Table 5 shows the Cd(II) adsorption capacities of some recently reported biosorbents. Different and superior to other biosorbents, the activated Firmiana Simplex Leaf has comparatively higher Cd(II) adsorption capacity and the fastest rate of reaction among the reported adsorbents. Also, as a widely distributed tree, the Firmiana Simplex provides a locally available, inexpensive source of adsorbent. The activation method provided here proved to be effective and appeared to be promising for the removal of heavy metals from wastewaters.

5. Conclusions

(1) Proper activation temperature (250 °C) helps to preserve the amine, carboxyl groups, and phosphate component, which are beneficial to Cd(II) adsorption. The Firmiana Simplex Leaf studied in this paper appeared prominent in Cd(II) removal from aqueous solution and exhibited promising potential for application in industry.
(2) The required duration for equilibrium was about 10 min while the initial Cd(II) concentration was raised from 50 to 200 mg L^{-1}, and the kinetics data were well fitted by the pseudo-first-order kinetics equation.
(3) The Langmuir model fits test data better than the Freundlich model or the D–R model. The Langmuir model predicted that the Cd(II) adsorption capacity of the AL adsorbent was 117.786 mg g^{-1}.
(4) The adsorption of Cd(II) on the AL adsorbent could be viewed as an endothermic and a preferential process with enthalpy change at around 25 kJ mol^{-1}. The negative Gibbs free energy changes indicated a spontaneous adsorption procedure.
(5) The optimum conditions for Cd(II) adsorption included: pH ≥ 6.0; dosage = 10 g L^{-1}; temperature ≥55 °C; and duration ≥10 min.
(6) The adsorption occurs between the cadmium ions and various species, including amine, carboxyl, phosphate, and quartz, all of which benefit the process.

Acknowledgement

References

[1] M. Gavrilescu, Removal of heavy metals from the environment by biosorption, Eng. Life Sci. 4 (2004) 219–232.
[2] A. Nakajima, T. Sakaguchi, Selective accumulation of heavy metals by microorganisms, Appl. Microbiol. Biotechnol. 24 (1986) 59–64.
[3] J.A. Scott, S.J. Palmer, J. Ingham, Decontamination of liquid streams containing cadmium by biomass adsorption, J. Chem. Electron. Symp. 96 (1986) 211–220.
[4] M.D. Mullen, D.C. Wolf, F.G. Ferris, T.J. Beveridge, C.A. Flemming, G.W. Bailey, Bacterial sorption of heavy metals, Appl. Environ. Microbiol. 55 (1989) 3143–3149.
[5] P.H. Kansenen, J. Venetvaara, Comparison of biological collectors of airborne heavy metals near ferrochrome and steelworks, Water Air Soil Pollut. 60 (1991) 337–359.
[6] D.E. Kimbrough, I.H. Suffer, Off-site forensic determination of airborne elemental emissions by multimedia analysis—a case study at 2 secondary lead smelters, Environ. Sci. Technol. 29 (1995) 2217–2221.
[7] E. Pip, Cd, Cu and Pb in soils and garden produce near a metal smelter at Flin-Flon, Manitoba, Bull. Environ. Contam. Toxicol. 46 (1991) 790–796.
[8] K. Kadirvelu, K. Thamaraiselvi, C. Namasivayam, Removal of heavy metals from industrial wastewaters by adsorption onto activated carbon prepared from an agricultural solid waste, Bioresour. Technol. 76 (2001) 63–65.
[9] M. Mohapatra, S. Anand, Studies on sorption of Cd(II) on Tata chromite mine overburden, J. Hazard. Mater. 148 (2007) 553–559.
[10] O. Kovalchuk, V. Titov, B. Hohn, L. Kovalchuk, A sensitive transgenic plant system to detect toxic inorganic compounds in the environment, Nature 19 (2001) 568–572.
[11] R.A. Anayurt, A. Sari, M. Tuzen, Equilibrium, thermodynamic and kinetic studies on biosorption of Pb(II) and Cd(II) from aqueous solution by macrofungus (Lactarius scrobiculatus) biomass, Chem. Eng. J. 151 (2009) 255–261.
[12] R. LeyvaRamos, J.R. RangelMendez, J. MendozaBarron, L. FuentesRubio, R.M. GuerreroCoronado, Water Sci. Technol. 35 (1997) 205–211.
[13] K. Bedoui, I. Bekri-Abbes, E. Srasra, Removal of cadmium(II) from aqueous solution using pure smectite and Lewatite S 100: the effect of time and metal concentration, Desalination 223 (2008) 269–273.
[14] P.A. Brown, S.A. Gill, S.J. Allen, Metal removal from wastewater using peat, Water Res. 34 (2000) 3907–3916.
[15] H.H. Tran, F.A. Roddick, J.A. O'Donnell, Comparison of chromatography and desiccant silica gels for the adsorption of metal ions-I. Adsorption and kinetics, Water Res. 33 (1999) 2992–3000.
[16] W.S. Peterlene, A.A. Winkler-Hechenleitner, E.A.G. Pineda, Adsorption of Cd(II) and Pb(II) onto functionalized formic lignin from sugar cane bagasse, Bioresour. Technol. 68 (1999) 95–100.
[17] M. Dakiky, M. Khamis, A. Manassra, M. Mer'eb, Selective adsorption of chromium(VI) in industrial wastewater using low-cost abundantly available adsorbents, Adv. Environ. Res. 6 (2002) 533–540.
[18] A. Sari, M. Tuzen, Kinetic and equilibrium studies of biosorption of Pb(II) and Cd(II) from aqueous solution by macrofungus (Amanita rubescens) biomass, J. Hazard. Mater. 164 (2–3) (2009) 1004–1011.
[19] K.A. Krishnan, T.S. Anirudhan, Removal of cadmium(II) from aqueous solutions by steam-activated sulphurised carbon prepared from sugar-cane bagasse pith: kinetics and equilibrium studies, Water SA 29 (2003) 147–156.
[20] K. Kadirvelu, C. Namasivayam, Activated carbon from coconut coirpith as metal adsorbent: adsorption of Cd(II) from aqueous solution, Adv. Environ. Res. 7 (2003) 471–478.
[21] K.K. Wong, C.K. Lee, K.S. Low, M.J. Haron, Removal of Cu and Pb by tartaric acid modified rice husk from aqueous solutions, Chemosphere 50 (2003) 23–28.
[22] K.S. Low, C.K. Lee, A.C. Leo, Removal of metals from electroplating wastes using banana pith, Bioresour. Technol. 51 (1995) 227–231.
[23] W.E. Marshall, E.T. Champagne, Agricultural by-products as adsorbents for metal ions in laboratory prepared solutions and in manufacturing wastewater, J. Environ. Sci. Health A 30 (1995) 241–261.
[24] S.H. Lee, J.W. Yang, Removal of copper in aqueous solution by apple wastes, Sep. Sci. Technol. 32 (1997) 1371–1387.
[25] Ontario Ministry of the Environment, Environmental risks of municipal non-hazardous waste landfilling and incineration, Queen's Printer for Ontario, 1999.
[26] X.W. Tang, Z.Z. Li, Y.M. Chen, Y. Wang, Removal of Cu(II) from aqueous solution by adsorption on Chinese Quaternary Loess: kinetics and equilibrium studies, J. Environ. Sci. Health A. 43 (2008) 779–791.
[27] D.D. Do, Adsorption Analysis: Equilibrium and Kinetics, Imperial College Press, London, 1998.
[28] O. Gulnaz, S.E. Saygideger, Study of Cu(II) biosorption by dried activated sludge: effect of physico-chemical environment and kinetics study, J. Hazard. Mater. 120 (2005) 193–200.
[29] D. DeNardis, D. Rosales-Yeomans, L.B.A. Philipossian, Characterization of copper-hydrogen peroxide film growth kinetics, Thin Solid Films 513 (2006) 311–318.
[30] G. Uslu, M. Tanyol, Equilibrium and thermodynamic parameters of single and binary mixture biosorption of lead (II) and copper (II) ions onto Pseudomonas putida: effect of temperature, J. Hazard. Mater. 135 (2006) 87–93.
[31] A. Sari, M. Tuzen, Biosorption of cadmium(II) from aqueous solution by red algae (Ceramium virgatum): equilibrium, kinetic and thermodynamic studies, J. Hazard. Mater. 157 (2008) 448–454.
[32] T. Akar, S. Tunali, I. Kiran, Botrytis cinerea as a new fungal biosorbent for removal of Pb(II) from aqueous solutions, Biochem. Eng. J. 25 (2005) 227–235.
[33] E.I. Unuabonah, K.O. Adebowale, B.I. Olu-Owolabi, Kinetic and thermodynamic studies of the adsorption of lead (II) ions onto phosphate-modified kaolinite clay, J. Hazard. Mater. 144 (2007) 386–395.
[34] F. Helfferich, Ion Exchange, McGraw-Hill, New York, 1962.
[35] J. Romero-Gonzalez, J.R. Peralta-Videa, E. Rodrıguez, S.L. Ramirez, J.L. Gardea-Torresdey, Determination of thermodynamic parameters of Cr(VI) adsorption from aqueous solution onto Agave lechuguilla biomass, J. Chem. Thermodyn. 37 (2005) 343–347.

[36] A. Saeed, M. Iqbal, M.W. Akhtar, Removal and recovery of lead(II) from single and multimetal (Cd, Cu, Ni, Zn) solutions by crop milling waste (black gram husk), J. Hazard. Mater. B 117 (2005) 65–73.

[37] A. Saeed, M.W. Akhtar, M. Iqbal, Removal and recovery of heavy metals from aqueous solution using papaya wood as a new biosorbent, Sep. Purif. Technol. 45 (2005) 25–31.

[38] N. Akhtar, J. Iqbal, M. Iqbal, Removal and recovery of nickel (II) from aqueous solution by loofa sponge-immobilized biomass of Chlorella sorokiniana: characterization studies, J. Hazard. Mater. B 108 (2004) 85–94.

[39] A. Saeed, M. Iqbal, Bioremoval of cadmium from aqueous solution by black gram husk (Cicer arientinum), Water Res. 37 (2003) 3472–3480.

[40] Y. Sag, T. Kutsal, Fully competitive biosorption of chromium(VI) and iron(III) ions from binary metal mixtures by R. arrhizus: use of the competitive Langmuir model, Process Biochem. 31 (1996) 573–585.

[41] A. Sari, M. Tuzen, M. Soylak, Adsorption of Pb(II) and Cr(III) from aqueous solution on Celtek clay, J. Hazard. Mater. 144 (2007) 41–46.

[42] X.W. Tang, Z.Z. Li, Y.M. Chen, Adsorption behavior of Zn(II) on calcinated Chinese loess, J. Hazard. Mater. 161 (2009) 824–834.

[43] Y.S. Ho, G. McKay, A comparison of chemisorption kinetic models applied to pollutant removal on various sorbents, Trans. Inst. Chem. Eng. 76B (1998) 332–340.

[44] X.W. Tang, Z.Z. Li, Y.M. Chen, Behaviour and mechanism of Zn(II) adsorption on Chinese loess at dilute slurry concentrations, J. Chem. Technol. Biotechnol. 83 (2008) 673–682.

[45] N. Tewari, P. Vasudevan, B.K. Guha, Study on biosorption of Cr(VI) by Mucor hiemalis, Biochem. Eng. J. 23 (2005) 185–192.

[46] Z. Aksu, O. Tunc, Application of biosorption for penicillin G removal: comparison with activated carbon, Process Biochem. 40 (2005) 831–847.

[47] S.H. Lin, R.S. Juang, Heavy metal removal from water by sorption using surfactant-modified montmorillonite, J. Hazard. Mater. B92 (2002) 315–326.

[48] O. Yavuz, Y. Altunkaynak, F. Guzel, Removal of copper, nickel, cobalt and manganese from aqueous solution by kaolinite, Water Res. 37 (2003) 948–952.

[49] Z. Jin, T. Akiyama, B.Y. Chung, Y. Matsumoto, K. Iiyama, S. Watanabe, Changes in lignin content of leaf litters during mulching, Phytochemistry 64 (2003) 1023–1031.

[50] R.A. Jones, Pyrrole studies. I. The infrared spectra of 2-monosubstituted pyrroles, Aust. J. Chem. 16 (1963) 93–100.

[51] M. Kılıç, M.E. Keskin, S. Mazlum, N. Mazlum, Hg(II) and Pb(II) adsorption on activated sludge biomass: effective biosorption mechanism, Int. J. Mineral Process. 87 (2008) 1–8.

[52] Y. Repelin, E. Husson, L. Abello, G. Lucazeau, Structural study of gels of V_2O_5: Normal coordinate analysis, Spectrochim. Acta A 41 (1985) 993–1003.

[53] K.D.O. Jackson, A guide to identifying common inorganic fillers and activators using vibrational spectroscopy, Internet J. Vib. Spectr. 2 (1998), http://www.ijvs.com/volume2/edition3/section3.html#jackson.

[54] J. Salas, Z. Benzo, G. González, Synthesis of hydroxyapatite by mechanochemical transformation, Rev. Latin Am. Met. Mat. 24 (2004) 12–16.

[55] A. Sinitsya, J. Copíkova, V. Prutyanov, S. Skoblya, V. Machovic, Amidation of highly methoxylated citrus pectin with primary amines, Carbohydr. Polymer. 42 (2000) 359–368.

[56] D. Mohan, K.P. Singh, Single- and multi-component adsorption of cadmium and zinc using activated carbon derived from bagasse—an agricultural waste, Water Res. 36 (2002) 2304–2318.

[57] W. Zheng, X.M. Li, F. Wang, Q. Yang, P. Deng, G.M. Zeng, Adsorption removal of cadmium and copper from aqueous solution by areca—a food waste, J. Hazard. Mater. 157 (2008) 490–495.

[58] S. Doyurum, A. Celik, Pb(II) and Cd(II) removal from aqueous solutions by olive cake, J. Hazard. Mater. B138 (2006) 22–28.

[59] N. Fiol, I. Villaescusa, M. Martinez, N. Miralles, J. Poch, J. Serarols, Sorption of Pb(II), Ni(II), Cu(II) and Cd(II) from aqueous solution by olive stone waste, Sep. Purif. Technol. 50 (2006) 132–140.

[60] F. Qin, B. Wen, X.Q. Shan, Y.N. Xie, T. Liu, S.Z. Zhang, S.U. Khan, Mechanisms of competitive adsorption of Pb, Cu, and Cd on peat, Environ. Pollut. 144 (2006) 669–680.